Development of a quorum-sensing based circuit for control of coculture population composition in a naringenin production system

Authors: Christina V. Dinh, Xingyu Chen, Kristala L. J. Prather

Corresponding author: Kristala L. J. Prather

Author affiliation: Department of Chemical Engineering, Massachusetts Institute of Technology, Cambridge, MA 02139

Abstract

As synthetic biology and metabolic engineering tools improve, it is feasible to construct more complex microbial synthesis systems that may be limited by the machinery and resources available in an individual cell. Co-culture fermentation is a promising strategy for overcoming these constraints by distributing objectives between sub-populations, but the primary method for controlling the composition of the co-culture of production systems has been limited to control of the inoculum composition. We have developed a quorum sensing (QS)-based growth-regulation circuit that provides an additional parameter for regulating the composition of a co-culture over the course of the fermentation. Implementation of this tool in a naringenin-producing co-culture resulted in a 60% titer increase over a system that was optimized by varying inoculation ratios only. We additionally demonstrated that the growth control circuit can be implemented in combination with a communication module that couples transcription in one sub-population to the cell-density of the other population for coordination of behavior, resulting in an additional 60% improvement in naringenin titer.

Keywords

Metabolic engineering, quorum sensing, co-culture fermentation

With more advanced understanding of cellular processes and improved synthetic biology tools, it is possible to design and construct systems that actuate increasingly complex cellular functions. In the context of metabolic engineering, these functions have resulted in an expansion in the set of molecules that can be produced through microbial synthesis and the types of production challenges that can be addressed. However, increasing complexity gives rise to potential problems such as growth burden or conflicting metabolic goals. To address situations in which achieving all design objectives in a single cell is not feasible, researchers have distributed functions between two or more strains in co-culture fermentations. For example, there have been a number of studies that partition metabolic pathways between sub-populations of a co-culture to alleviate metabolic burden in individual cells^{1–8}. Co-culture fermentations additionally offer strain construction advantages, allowing for more independent optimization of modules in separate strains and mitigating concerns for unpredictable interactions between the modules.

In some pathways, co-culturing could be a strategy for overcoming enzyme inhibition by an intracellular intermediate or product. One such example is the naringenin pathway that is commonly assembled in E. coli⁹⁻¹². This pathway converts L-tyrosine and malonyl-CoA to naringenin using four heterologous enzymes. Tyrosine ammonia lyase (TAL) converts tyrosine to p-coumaric acid, which is converted to coumaryl-CoA by 4-coumaryl-CoA ligase (4CL). Chalcone synthase (CHS), and chalcone isomerase (CHI) then convert coumaryl-CoA to naringenin (Figure S1). Results from previous studies suggest that efficient naringenin production in this pathway is limited by inhibition of TAL by coumaryl-CoA. While most efforts to overcome this limitation have been focused on preventing accumulation of coumaryl-CoA by delaying its production or by flux balancing, this problem could also be addressed by separating TAL and coumaryl-CoA in different sub-populations. Such a system would contain one strain that expresses TAL to convert tyrosine to p-coumaric acid, which exits the cell, and a second strain which expresses 4CL, CHS, and CHI to convert p-coumaric acid to naringenin. Since coumaryl-CoA is retained in the second strain, accumulation does not hinder the activity of TAL contained in the first strain. This approach was employed previously by Jones et al. to produce naringenin as part of an anthocyanin-producing polyculture⁴, and Ganesan et al. improved naringenin production by implementing a similar strategy in which one strain produces both tyrosine and p-coumaric acid for uptake in a second strain that expresses the entire naringenin pathway⁸.

Co-culture fermentation studies have shown that the relative sub-population size is an important parameter^{2,4–8,13}, but control of this key parameter in co-culture systems has so far been limited to varying the inoculation ratio, forcing the user to define the composition profile for the entire fermentation with one parameter. In nature, microbial cells alter their metabolism in response to the cell density of both their own and other communicating species through quorum-sensing (QS) circuits. Members of a population excrete signaling molecules such that the concentration of these molecules is coupled to the cell-density of that sub-population. Neighboring cells containing the appropriate circuitry can then sense the presence of the signaling molecule. In the canonical *lux*

QS circuit, the signaling molecule (N-acyl homoserine lactone, AHL) binds to the regulator protein LuxR, and this AHL-bound LuxR complex activates transcription from the P_{lux} promoter. QS promoters such as the P_{lux} promoter control expression of the genes associated with cell-density-dependent behavior.

We and others have implemented QS circuits to coordinate cellular behavior in mono- and cocultures. For example, metabolic fluxes can be coupled to cell-density by placing genes which encode for key enzymes under control of QS promoters^{14–17}. In the context of microbial synthesis, QS circuits offer a pathway-independent and autonomous method for dynamic control, which may be more industrially feasible than exogenous chemical addition. You et al. showed that cellular growth rates can be dynamically down-regulated by placing a gene encoding a toxic protein under control of a QS promoter¹⁸ and Stephens et al. showed dynamic up-regulation of cellular growth rate by QS-mediated regulation of *ptsH* in a knockout strain background¹⁹. These ideas have been applied to co-culture systems to facilitate communication between sub-populations, resulting in coordinated expression or growth behavior, although these tools have not yet been applied to microbial synthesis systems^{19–26}.

We aimed to develop a QS-based growth-regulation circuit that would provide an additional parameter to control co-culture composition profiles. This circuit down-regulates growth rate by decreasing glycolytic flux with increasing cell density. The relationship between cell-density and growth down-regulation can be tuned by varying the expression level of the AHL synthase to give varied co-culture dynamics with the same inoculation ratio. We applied the circuit towards regulating population compositions in a naringenin-producing co-culture to achieve a significant improvement over the optimal co-culture that lacks the control circuit. The growth down-regulation circuit was then implemented in combination with a communication module in which the cell-density of one sub-population regulates transcription of a regulatory module in the other to show how these strategies can be used in combination to improve co-culture synthesis systems.

Results and discussion

Growth control circuit

To construct a QS-based circuit which dynamically down-regulates growth rate in response to increasing cell density, we modified a circuit previously developed in our group. Brockman and Prather developed a circuit that dynamically down-regulates glycolytic flux with the goal of accumulating glucose-6-phosphate by controlling phosphofructokinase (Pfk) levels²⁷. They placed *pfkA* under control of a constitutive synthetic promoter and appended the gene with an SspB-dependent degradation tag such that Pfk-1 is degraded upon *sspB* expression. The background strain (IB1643) additionally contained knockouts of *pfkB*, *zwf*, and *sspB* to achieve tight regulation,

and a new copy of sspB was introduced under the control of a small molecule (anhydrotetracycline, aTc) inducible promoter. The circuit was intended to be a glycolytic flux control system, which resulted in a titratable growth down-regulation effect with increasing sspB expression when cells were grown in minimal medium with glucose as the sole carbon source²⁷.

To obtain a QS-based system for autonomous and dynamic growth control, we integrated a *lux* QS circuit, which contains *luxR* under the control of a constitutive promoter and *sspB* under the P_{lux} promoter and an RBS library, into a variant of IB1643 that contains the DE3 lysogen (IB1643(DE3)) (Figure 1A). We screened the resulting RBS variants for the desired phenotype of growth rate down-regulation with AHL addition, with maintenance of a fast growth rate in the absence of AHL. The strain selected (IB1643(DE3)-lux) showed AHL-dependent growth behavior in which AHL addition at inoculation or during mid-exponential phase exhibits a decreased growth rate (Figure 1B). We then integrated a library of *esaI* expression levels into IB1643(DE3)-lux to make the IB1643(DE3)-LXX strain series. Based on previous characterization, we expect that increasing *esaI* expression leads to faster production of AHL, resulting in stronger growth down-regulation effects at lower cell-densities¹⁶. An estimation of the specific growth rate of the IB1643(DE3)-LXX strain series at mid-exponential phase confirms this trend (Figure 1C).

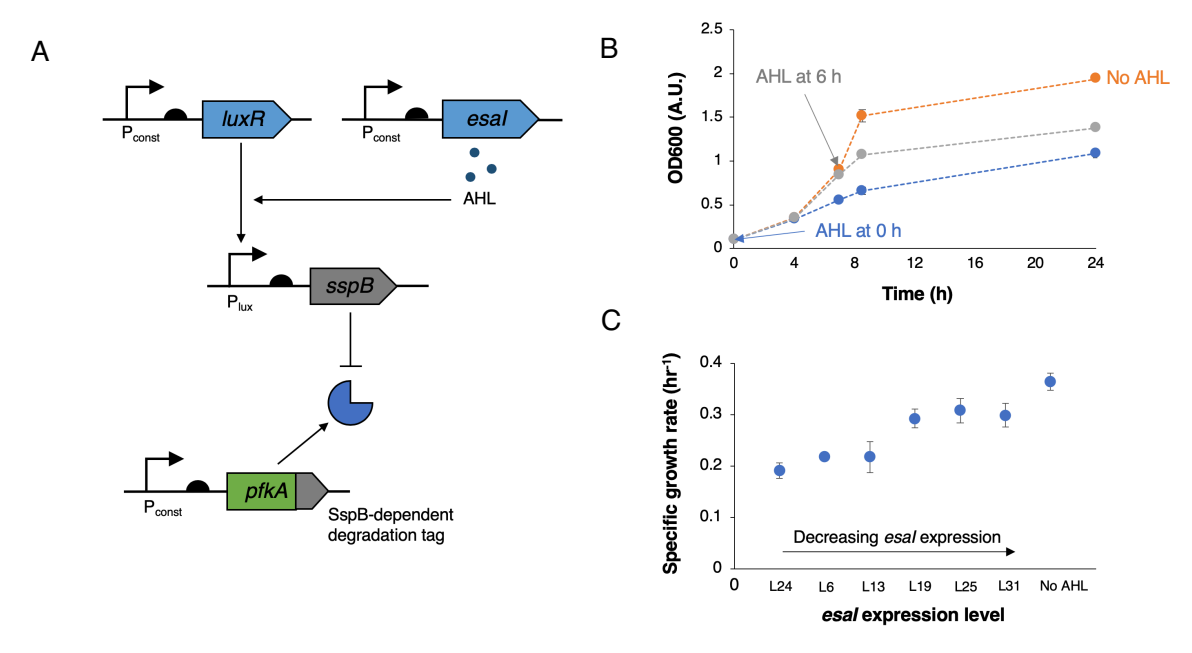


Figure 1. Growth regulation circuit and characterization. (**A**) Diagram of the growth regulation circuit. The native copy of *pfkA* is under control of a synthetic constitutive promoter and appended with an SspB-dependent degradation tag. The only copy of *sspB* is under control of the P_{lux} promoter, which is activated by AHL-bound LuxR. AHL is produced in a cell-density dependent manner though constitutive expression of *esaI*. The background strain contains knockouts of *sspB*, *zwf*, and *pfkB*. (**B**) Growth curves of IB1632(DE3)-lux with various AHL treatments. AHL addition at inoculation or during mid-exponential phase results in decreased growth rate. (**C**) Effect of *esaI* expression level on the specific growth rate of strains containing the growth regulation circuit during mid-exponential phase. Each data point represents the growth rate of a strain with a different level of *esaI* expression (variant indicated on x-axis). Increasing *esaI* expression generally results in decreased specific growth rate. Error bars represent the s.d. of triplicate trials.

Co-culture population characterization

Next, we evaluated whether the growth regulation circuit could offer a method for regulating coculture population dynamics. All co-cultures tested contain an RFP-expressing strain (Strain R, BL21(DE3) + pTrc-RFP), and a GFP-expressing strain containing the growth regulation circuit (Strain G, IB1643(DE3)-lux or IB1643(DE3)-LXX + pTrc-GFP). With this regulation scheme, we expected that each strain would initially grow at its baseline rate, or the rate without AHL, until a sufficient concentration of AHL accumulates, resulting in down-regulation in the growth rate of Strain G (Figure 2A). A time course study of the population dynamics shows that at every inoculation ratio tested, the presence of EsaI results in a lower fraction of Strain G by 24 hours, and final population compositions correlate well with the predicted *esaI* expression levels (Figure 2B).

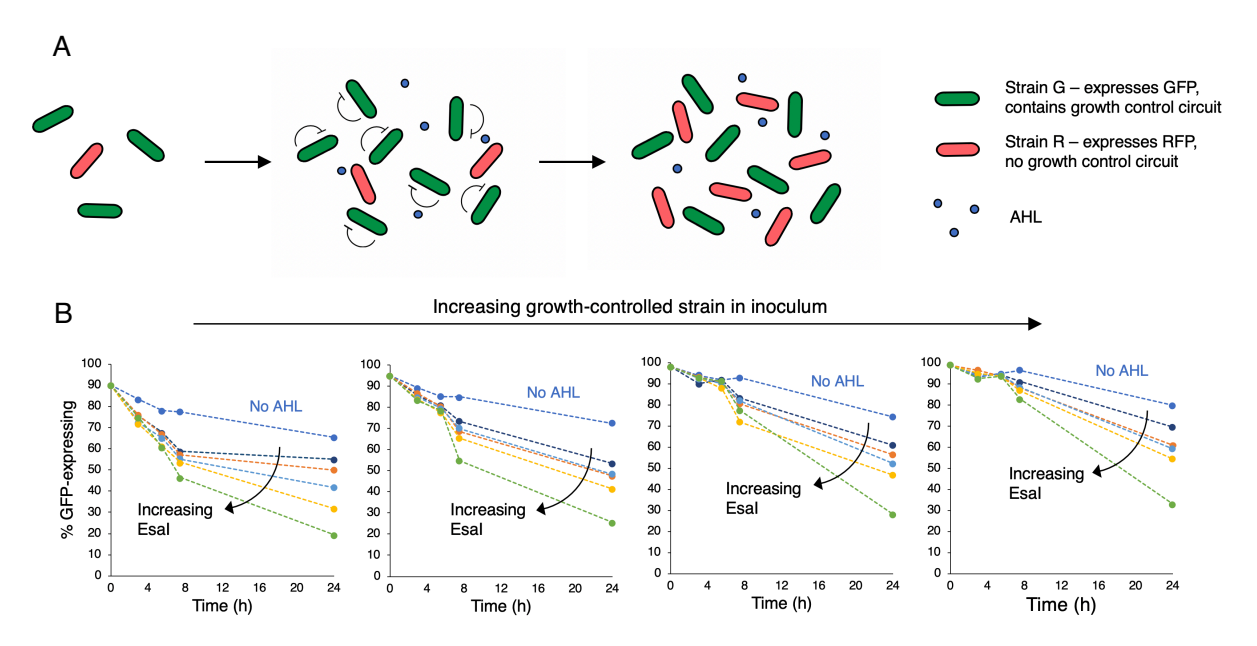


Figure 2. Effect of the growth regulation circuit in a co-culture. (**A**) Illustration of the different stages of the co-culture fermentation in which the GFP-expressing strain (Strain G) contains the growth regulation circuit. At low cell density, both strains will grow at their baseline rates. Once the culture has accumulated a certain concentration of AHL, corresponding to a cell-density of Strain G, the growth rate of the green sub-population slows down. At the end of the fermentation, Strain R represents a greater fraction of the population than it would in the absence of growth regulation. (**B**) Representative population profiles for co-culture of varying inoculation compositions (L to R: 90%, 95%, 98%, and 99% Strain G) and *esal* expression levels (different curves). For all inoculation ratios, increasing the *esa* expression level leads to a smaller fraction of Strain G by 24 h.

Growth rate control in the naringenin pathway

We then applied the growth control circuit to a naringenin-producing co-culture system to demonstrate how this additional control parameter can result in more favorable population dynamics to improve production. The co-culture naringenin production system includes one strain (Strain 1) that expresses *TAL* (pET-*TAL-GFP*) to convert L-tyrosine to *p*-coumaric acid and GFP for tracking population composition, and a second strain (Strain 2) that expresses *4CL*, *CHS*, and *CHI* (pCOLA-*4CL* and pET-*CHS-CHI*) to convert *p*-coumaric acid to naringenin. Since we hypothesized that successful co-cultures would contain relatively high levels of Strain 2 by the end of the fermentation, we implemented the growth control circuit with varying *esaI* expression levels in Strain 1 (Figure 3A).

To search for efficient naringenin producers, we co-cultured the Strain 1 *esaI* library with Strain 2 at varying inoculation ratios. Analysis of the final co-culture composition confirms that the trends between *esaI* expression level and composition seen in Figure 2B still hold in this context (Figure S2). Characterization of the final co-culture composition and titers shows that *p*-coumaric acid titer increases with the fraction of Strain 1 as expected (Figure 3B). The relationship between naringenin titer and co-culture composition suggests that the most efficient production relies on achieving a balance between *p*-coumaric acid production and consumption capabilities. Cultures containing low levels of Strain 1 are limited by low *p*-coumaric acid production rates while cultures with low levels of Strain 2 are limited by their low rates of *p*-coumaric acid conversion to naringenin (Figure 3C).

To evaluate impact of the growth regulation circuit on production, we compared naringenin titers from co-cultures with and without the growth control circuit. The variant of Strain 1 used for the "without growth circuit" sample has the same genetic background as the "with growth circuit" strains, but lacks *esaI* such that the Pfk degradation rate is low and constant. When this variant of Strain 1 was co-cultured with Strain 2 at varying inoculation ratios, the best sample produced 0.1 mM naringenin (Figure 3B and Figure S3C), about 60% less than the top naringenin production system which employed the growth regulation circuit. This result suggests that the additional control parameter is beneficial in this context (Figure 5, bars 2 and 5). The composition of the optimal "no growth control" sample increases from 5% to 29% Strain 1 whereas the composition of the optimal strain with growth control decreases from 40% to 21% Strain 1 over the course of the fermentation. We hypothesize that a higher starting fraction of Strain 1 in the growth-controlled sample corresponds to earlier *p*-coumaric acid production, leading to more effective conversion by Strain 2.

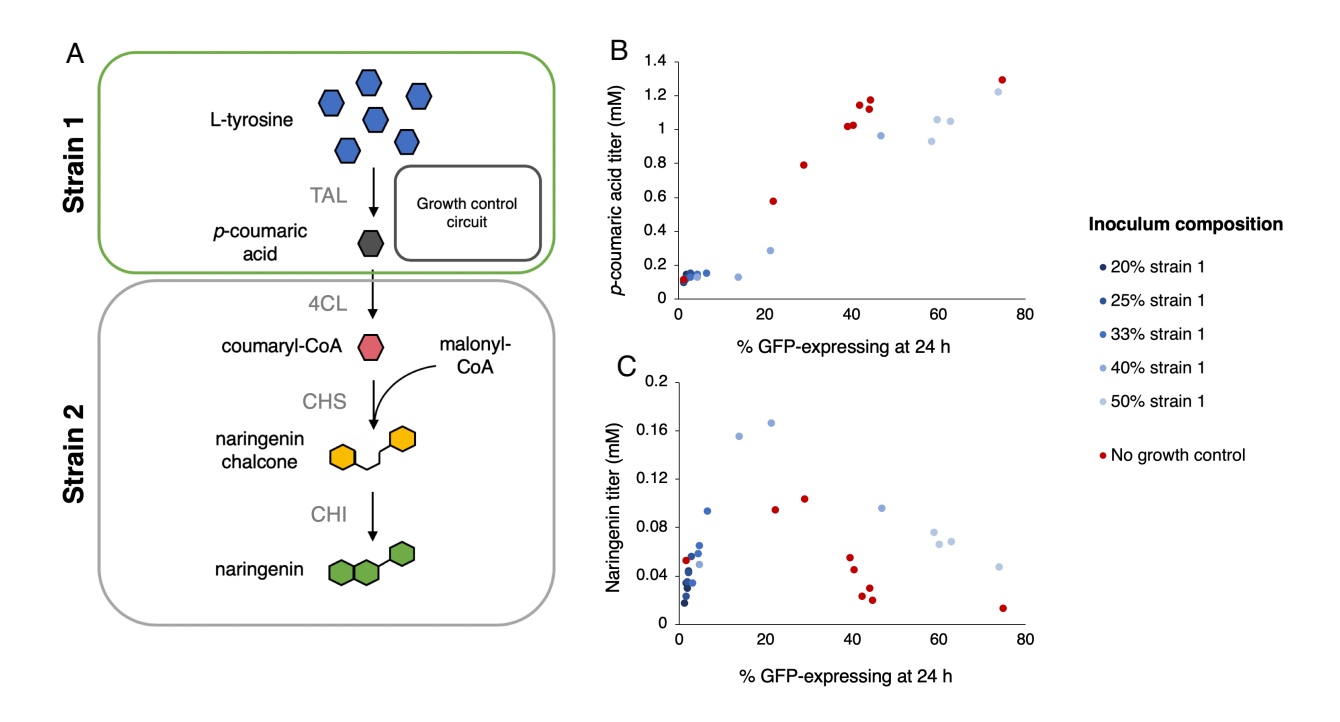


Figure 3. Naringenin co-culture system with growth regulation. (**A**) Illustration of the sub-populations in the naringenin co-culture system. Strain 1 contains the growth control circuit (IB1643(DE3)-LXX) and constitutively expresses *TAL* and *GFP*. Strain 2 is BL21(DE3) with constitutively expressed *4CL*, *CHS*, and *CHI*. (**B**) *p*-Coumaric acid titers as function of the co-culture composition at 24 h. Data points with the same shade of blue represent samples in which Strain 1 contains different *esaI* expression levels, but the inocula contain the same fractions of Strains 1 and 2. Red data points represent samples in which Strain 1 does not contain *esaI*, inoculated at varying compositions. Increasing the fraction of Strain 1 in the co-culture results in increased *p*-coumaric acid titers. (**C**) Naringenin titers as a function of the co-culture composition at 24 h. The intermediate fractions of Strain 1 in the co-culture results in the best naringenin production levels.

Growth rate control with sub-population communication in naringenin pathway

The maximum pathway flux in the co-culture system may be limited by the fact that each gene is only expressed in a fraction of the population. To evaluate the impact of this feature, we benchmarked the top co-culture naringenin titer against two relevant mono-culture controls. As previously mentioned, TAL inhibition is commonly addressed by delaying expression of TAL and 4CL, with the goal of ensuring that downstream pathway enzymes (CHS and CHI) are present first, to minimize the accumulation of the intermediate p-coumaroyl-CoA. This approach is subject to a different limitation in which there is low pathway flux early on in the fermentation before induction of TAL and 4CL expression. In previous work, we controlled TAL and 4CL expression under P_{esaR} promoters which are de-repressed in the presence of AHL. A screen of esaI expression levels corresponding to different TAL and 4CL induction times identified a top strain that produces 0.17 mM naringenin (Figure 5, bar 4)¹⁶. To study a naringenin production system that is free of both limitations, we cultured Strain 2 (BL21(DE3) + pCOLA-4CL + pET-CHS-CHI) with varying

concentrations of fed *p*-coumaric acid supplied in the culture medium. This system, which is not limited by a fermentation phase with low pathway flux, *p*-coumaric acid levels, or the fraction of Strain 2, produced 0.18 mM naringenin at the optimal concentration of fed *p*-coumaric acid (Figure 5, bar 3 and Figure S4).

The different methods for overcoming TAL inhibition in the naringenin pathway (fed p-coumaric acid, delay of coumaryl-CoA production, and co-culture) result in naringenin titers that are not significantly different (Figure 5, bars 3-5). This observation led us to hypothesize that implementation of these strategies leads to a more significant limitation elsewhere in the pathway, likely the malonyl-CoA-dependent step based on previous studies^{28–30}. Our group and others have addressed the malonyl-CoA limitation by expressing silencing components to down-regulate TCA cycle and fatty acid synthesis pathways that consume the substrate^{10,12,16}. However, altering these endogenous metabolic fluxes can result in undesired growth effects and thus, it is preferable to delay expression of the down-regulation system until the appropriate point in the fermentation, possibly once a sufficient concentration of p-coumaric acid is reached.

Since the p-coumaric acid concentration is expected to strongly correlate with the cell-density of Strain 1, we can implement a QS circuit in Strain 2 to regulate expression of silencing components for malonyl-CoA accumulation. To confirm that the AHL produced from Strain 1 is able to trigger expression from the P_{lux} promoter in a different sub-population, the Strain 1 esal library was cocultured with BL21(DE3) with mCherry controlled under the lux QS circuit. Analysis of the RFP fluorescence profiles confirmed that the AHL produced from the Strain 1 sub-population is able to trigger expression from the P_{lux} promoter in a second sub-population in an EsaI level-dependent manner (Figure S5). In a previous study, we improved a mono-culture naringenin production system by controlling expression of CRISPRi components under a lux QS circuit for the purpose of increasing malonyl-CoA availability. A screen of gene target combinations and switching dynamics identified a best producer that targeted the endogenous genes, fabF and sucC, and employed the strongest luxR expression level¹⁶. We implemented this top silencing system in Strain 2 by transforming plasmids containing dCas9 and sgRNA under Plux promoters (pACYC-P_{lux}-dCas9-P_{con}-RBS4-luxR and pCDF-P_{lux}-sg(fabF-sucC)) into Strain 2. By incorporating this additional circuit, increasing cell-density of Strain 1 results in both growth down-regulation of Strain 1 and expression of CRISPRi components in Strain 2 for malonyl-CoA accumulation (Figure 4A).

To again screen for top naringenin producers, the Strain 1 *esaI* library and Strain 2 with the CRISPRi modules were co-cultured with varying inoculation ratios. Analysis of final composition trends showed that within inoculation ratios, increasing *esaI* expression levels resulted in an increased fraction of Strain 1 (Figure S6), suggesting that *fabF* and *sucC* down-regulation has a stronger negative growth effect than Pfk degradation. Although both modules are controlled under *lux* QS circuits, the relative growth effects can be tuned independently by varying the expression

level of *luxR* in each strain. This is a promising tuning parameter for further expanding the range of composition profiles, which could potentially lead to additional production benefits. In general, *p*-coumaric acid titers again increase with increasing fractions of Strain 1 at stationary phase (Figure 4B) and the naringenin titer dependence on the population composition again indicates a trade-off between *p*-coumaric acid production and consumption capabilities (Figure 4C), although the balance has shifted to favor higher fractions of Strain 1.

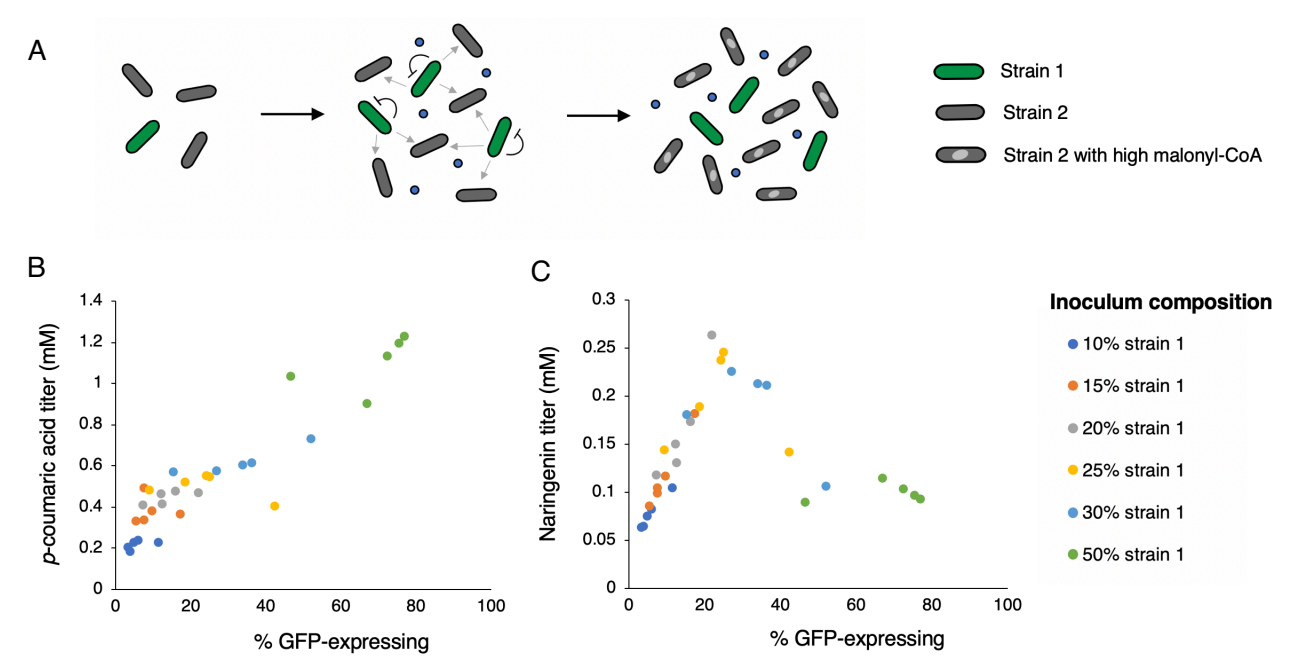


Figure 4. Naringenin co-culture system with growth regulation and malonyl-CoA accumulation. (**A**) Illustration of the different stages of the co-culture system. At low cell-densities, both strains grow at their baseline rates. As the cells grow, the AHL concentration in the media increases with the cell-density of Strain 1, resulting in decreased growth rate of Strain 1 and expression of CRISPRi components in Strain 2 for malonyl-CoA accumulation. (**B**) *p*-Coumaric acid titers as a function of the percentage of GFP-expressing cells (Strain 1) in the co-culture. Data points with the same color represent samples in which Strain 1 contains different *esaI* expression levels, but the inocula contain the same fractions of Strains 1 and 2. Generally, increasing the fraction of Strain 1 at stationary phase results in increased *p*-coumaric acid titers. (**C**) Naringenin titers as a function of the fraction of Strain 1 at stationary phase. High naringenin titers occur when neither strain dominates the co-culture.

Comparison of naringenin production systems

To summarize, constitutive expression of all naringenin pathway genes in a mono-culture suffers from poor production due to TAL inhibition by coumaryl-CoA, which can be relieved through a co-culture approach to separate TAL and coumaryl-CoA to give a 6-fold increase in naringenin titer (Figure 5, bars 1 and 2). Implementation of a growth control circuit into one of the co-culture strains (Strain 1) allows for an additional parameter for tuning population dynamics, resulting in a 60% increase in naringenin titers over the titers without this control capability (Figure 5, bars 2 and 5). These titers are comparable to the ones achieved by feeding *p*-coumaric acid to Strain 2

and by delaying production of coumaryl-CoA in a mono-culture, demonstrating the efficacy of the co-culture strategy with growth control (Figure 5, bars 3 and 4). To further increase naringenin titers, we implemented a CRISPRi-mediated down-regulation module which responds to the cell-density of the *p*-coumaric acid producing strain, resulting in an additional 60% increase in naringenin titers (Figure 5, bars 5 and 6).

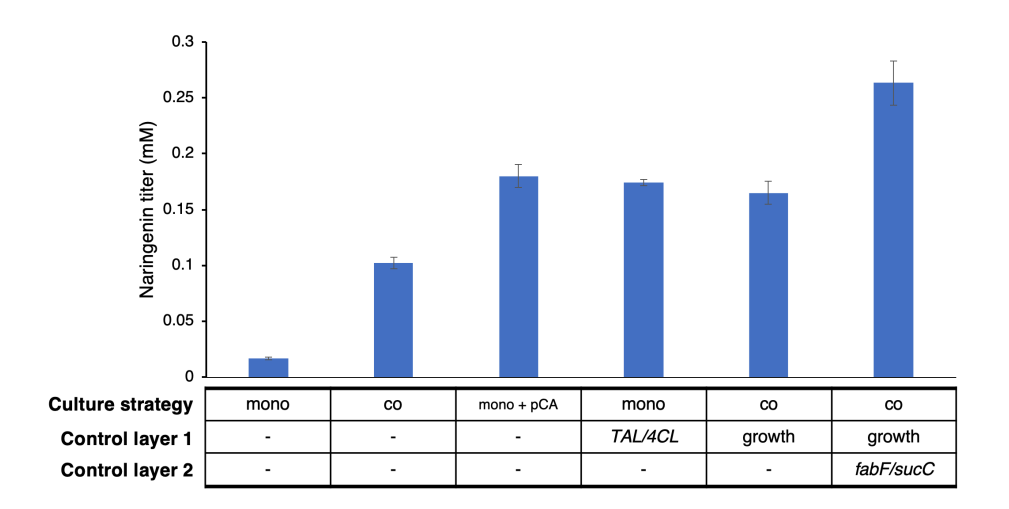


Figure 5. Comparison of various naringenin production systems. The titer shown for the mono-culture strategy without dynamic control represents the titer that results from high constitutive expression of all naringenin pathway genes (bar 1). The titer shown for the co-culture strategy with no dynamic control is the highest titer achieved by varying inoculation ratios only using a Strain 1 variant that lacks Esal (bar 2; Figure S3C). The titer shown for the mono-culture with added *p*-coumaric acid strategy is the highest titer achieved by varying fed *p*-coumaric acid concentrations supplied in a mono-culture of Strain 2 (bar 3; Figure S3). The titer shown for the mono-culture with *TAL/4CL* control is highest titer achieved by controlling *TAL* and *4CL* expression from P_{esaR-H} promoters and varying *esal* expression levels (bar 4). The two right-most bars are the top titers shown in Figures 3C and 4C (bars 5 and 6).

In conclusion, co-culturing presents a promising solution for overcoming the physiological limitations imposed by individual cells. In the context of metabolic engineering, previous studies have demonstrated the importance of co-culture composition for achieving efficient production, but co-culture composition during the entire fermentation is commonly controlled only by the inoculum composition. With the aim of obtaining greater control over the population dynamics of a co-culture, we developed a QS-based circuit that down-regulates the growth rate of a sub-population in response to an increase in its own cell-density in a tunable manner. Application of this system to a naringenin-producing co-culture resulted in an expansion of the range of possible population dynamics, which led to a significant increase in titer compared to an uncontrolled sample. We then implemented a second QS module to facilitate coordination between sub-population size and malonyl-CoA accumulation to achieve additional production improvements. To our knowledge, this is the first application of QS-based control tool for composition regulation in a co-culture production system.

Materials and Methods

All strains and plasmids used in this study are summarized in Tables S1 and S2, respectively. Sequences for promoters and RBS sequences are provided in Table S3. For plasmid construction and gene/genome editing, cells were cultured in Luria-Bertani (LB) broth at either 30 or 37 °C. Temperature-sensitive plasmids were cured at 42 °C.

Strain construction

Genomic integrations. The λDE3 expression cassette with T7 RNA polymerase under the lacUV5 promoter was integrated into strain IB1643²⁷ using "clonetegration"³¹. The DE3 expression cassette was amplified from the genome of BL21(DE3) using primers DE3_fwd and DE3_rev and inserted into the pOSIP-KT backbone using restriction digestion and ligation. The ligation product was used to transform *E. coli* strain IB1643 for integration into the P21 locus. The phage integration genes and antibiotic resistance cassette were cured by transforming with a plasmid containing FLP under control of the P_{tet} promoter (pTet-FLP) yielding strain IB1643(DE3). An *sspB* expression library containing constitutive *luxR* and *sspB* under the P_{lux} promoter was then integrated into the HK022 locus of IB1643(DE3) using "clonetegration" yielding strain IB1643(DE3)-RBSX-lux. The expression cassettes were digested from the pACYC-P_{con}-luxR-P_{lux}-RBSX-sspB series and ligated into pOSIP-KH for transformation into IB1643(DE3). The *esa1* expression cassette was integrated into the genome of IB1643(DE3)-RBS2-lux (renamed IB1643(DE3)-lux) under a several different constitutive synthetic promoters (Table S3)¹⁴ via "clonetegration" to yield the IB1643(DE3)-LXX strain series.

sspB expression plasmids. The pACYC-P_{con}-luxR-P_{lux}-RBSX-sspB strain series was constructed using a Golden Gate Assembly reaction containing a pACYC-P_{con}-luxR-P_{lux}-2xBbsI-sspB plasmid and annealed oligos containing the RBS sequence library and the appropriate sticky ends. pACYC-P_{con}-luxR-P_{lux}-2xBbsI-sspB was constructed using Golden Gate Assembly with the backbone fragment amplified from pACYC-duet using primers Lux_sspB1 a Lux_sspB2, the luxR, P_{lux}, and sspB terminator fragments amplified from pSB1A2-P_{con}-luxR-P_{lux}-GFP³² using primers Lux_sspB3-6, 9 and 10, and the sspB gene amplified from the genome of MG1655 using primers Lux_sspB7 and Lux_sspB8.

Naringenin pathway. Plasmid pETM6-TAL-GFP was constructed using Golden Gate Assembly. Primers TAL_GFP1 – TAL_GFP4 were used to amplify PCR fragments from pETM6-TAL (Addgene plasmid # 100947)⁴ – a gift from Mattheos Koffas (Rensselaer Polytechnic Institute, Department of Chemical and Biological Engineering) – and primers TAL_GFP5 and TAL_GFP6 were used to amplify fragments from pET-GFP³². The pCOLA-4CL plasmid was constructed

using restriction digest and ligation cloning using primers 4CL_CC1 and 4CL_CC2 to amplify the 4CL gene from pCOLA-P_{esaR-H}-TAL-4CL¹⁶.

Culturing and fermentations

Fluorescence characterization. Switching dynamics of the lux QS circuit over varying esal expression levels were quantified using the BioLector microbioreactor system (m2p-labs, Baesweiler, Germany). Individual colonies were inoculated in LB medium and grown overnight at 30 °C. 1 mL cultures were inoculated from these seeds at OD₆₀₀ 0.05 into BioLector 48-well flower plates and incubated at 30 °C, 1200 rpm (3 mm orbit), and 80% relative humidity. The plate was sealed with a gas-permeable sealing foil (m2p-labs). Cultures were monitored for OD (BioLector units) and RFP fluorescence over time.

Growth characterization. Individual colonies were inoculated in 3 mL LB broth and grown overnight at 30 °C, then diluted 1:100 into 3 mL MOPS minimal medium containing 5 g/L glycerol, 500 mg/L tyrosine, 4 g/L NH₄Cl, 1 g/L K₂HPO₄, 2 mM MgSO₄, 0.1 mM CaCl₂, 40 mM MOPS, 4 mM Tricine, 50 mM NaCl, 100 mM Bis-Tris, 143 uM EDTA, 31 uM FeCl₃, 6.2 uM ZnCl₃, 0.76 uM CuCl₂. 0.42 uM CoCl₂, 1.62 uM H₃BO₃ and 0.081 uM MnCl₂ at 30 °C for ~6 h. These were used to inoculate into 5 mL working cultures of MOPS minimal medium containing 5 g/L D-glucose at OD₆₀₀ 0.1. Samples were taken periodically for quantification of cell density and relative population size until 24 h. Specific growth rates were estimated when the cultures reached an OD₆₀₀ of 0.5, which occurred between 4-8 h for all samples.

Fermentations. Naringenin production trials were performed in glass vials with 5 mL working volume at 30 °C and 80% humidity with 250 rpm shaking in modified MOPS minimal medium containing 5 g/L D-glucose, 500 mg/L tyrosine, 4 g/L NH₄Cl, 1 g/L K₂HPO₄, 2 mM MgSO₄, 0.1 mM CaCl₂, 40 mM MOPS, 4 mM Tricine, 50 mM NaCl, 100 mM Bis-Tris, 143 uM EDTA, 31 uM FeCl₃, 6.2 uM ZnCl₃, 0.76 uM CuCl₂. 0.42 uM CoCl₂, 1.62 uM H₃BO₃ and 0.081 uM MnCl₂. For strains containing plasmids with pET, pCOLA, pACYC, and pCDF vector backbones, the medium was also supplemented with 100 μg/mL carbenicillin, 50 μg/mL kanamycin, 34 μg/mL chloramphenicol, and 100 μg/mL spectinomycin, respectively, for plasmid maintenance. Strains were initially grown in 3 mL of LB medium at 30 °C overnight, then diluted 1:100 into 3-mL seed cultures of modified MOPS medium with 5 g/L glycerol for ~6 h at 30 °C. These were used to inoculate working cultures at OD₆₀₀ 0.1. Samples were taken periodically for quantification of cell density, relative population size, and extracellular metabolites. Fermentations were carried out for 48 hours.

Estimation of relative population sizes

Relative population sizes within co-cultures were estimated using fluorescence assisted cell sorting (FACS). 1-10 μ L of cell culture was suspended in 1 mL of PBS and stored at 4 °C until analysis. FACS screening was performed on a FACS LSRII (Becton Dickinson) at the Koch Institute Swanson Biotechnology Center Cytometry Core facility (Cambridge, MA).

Quantification of metabolites

Tyrosine, *p*-coumaric acid, and naringenin were quantified by high performance liquid chromatography (HPLC) on an Agilent 1100 series instrument (Santa Clara, CA) with a ZORBAX Eclipse column (4.6 mm x 150 m x 3.5 um). The HPLC was run with a mixture of solution A (water + 0.1% TFA) and solution B (acetonitrile + 0.1% TFA) as the eluent at a flow rate of 1 mL/min. The following gradient was used: at 0 min, 90% solution A and 10% solution B, by 10 min, 60% solution A and 40% solution B, by 15 min, 40% solution A and 60% solution B, by 15.5 min, 0 % solution A and 100% solution B, 15.5 – 21 min, 0 % solution A and 100 % solution B, by 21.5 min, 90% solution A and 10% solution B, 21.5 – 28 min, 90% solution A and 10% solution B. Compounds were quantified with 10 μL injections using diode-array detection at 270 nm (tyrosine) or 290 nm (*p*-coumaric acid and naringenin).

Statistics

All error bars are reported as standard deviations of replicates. The number of replicates is provided in the corresponding figure caption.

Acknowledgments

This work was supported by the US National Science Foundation through the Division of Molecular and Cellular Biosciences (Grant No. MCB-1817708).

Supporting Information

Supplemental figures including the chemical structures of the compounds in the naringenin pathway (Figure S1), co-culture composition data from Figure 4B-C resolved by strain (Figure S2), additional data on co-culture fermentations without growth control (Figure S3), naringenin titers with varying *p*-coumaric acid feed concentrations (Figure S4), characterization of QS-

mediated cross-activation (Figure S5), and co-culture composition data from Figure 4B-C resolved by strain.

Supplemental tables including a list of strains and their corresponding genotypes (Table S1), plasmids and their corresponding genotypes (Table S2), promoter and RBS sequences (Table S3), and primer sequences (Table S4).

References

- (1) Shin, H.-D.; McClendon, S.; Vo, T.; Chen, R. R. Escherichia Coli Binary Culture Engineered for Direct Fermentation of Hemicellulose to a Biofuel. *Appl. Environ. Microbiol.* **2010**, *76* (24), 8150 LP 8159. https://doi.org/10.1128/AEM.00908-10.
- Tsai, S.-L.; Goyal, G.; Chen, W. Surface Display of a Functional Minicellulosome by Intracellular Complementation Using a Synthetic Yeast Consortium and Its Application to Cellulose Hydrolysis and Ethanol Production. *Appl. Environ. Microbiol.* **2010**, *76* (22), 7514 LP 7520. https://doi.org/10.1128/AEM.01777-10.
- (3) Zhou, K.; Qiao, K.; Edgar, S.; Stephanopoulos, G. Distributing a Metabolic Pathway among a Microbial Consortium Enhances Production of Natural Products. *Nat. Biotechnol.* **2015**, *33*, 377.
- (4) Jones, J. A.; Vernacchio, V. R.; Collins, S. M.; Shirke, A. N.; Xiu, Y.; Englaender, J. A.; Cress, B. F.; McCutcheon, C. C.; Linhardt, R. J.; Gross, R. A.; et al. Complete Biosynthesis of Anthocyanins Using E. Coli Polycultures. *MBio* **2017**, *8* (3), 1–9. https://doi.org/10.1128/mBio.00621-17.
- (5) Zhang, H.; Stephanopoulos, G. Co-Culture Engineering for Microbial Biosynthesis of 3-Amino-Benzoic Acid in Escherichia Coli. *Biotechnol. J.* 2016, 11 (7), 981–987. https://doi.org/10.1002/biot.201600013.
- (6) Ahmadi, M. K.; Fang, L.; Moscatello, N.; Pfeifer, B. A. E. Coli Metabolic Engineering for Gram Scale Production of a Plant-Based Anti-Inflammatory Agent. *Metab. Eng.* **2016**, *38*, 382–388. https://doi.org/https://doi.org/10.1016/j.ymben.2016.10.001.
- (7) Li, Z.; Wang, X.; Zhang, H. Balancing the Non-Linear Rosmarinic Acid Biosynthetic Pathway by Modular Co-Culture Engineering. *Metab. Eng.* **2019**, *54*, 1–11. https://doi.org/https://doi.org/10.1016/j.ymben.2019.03.002.
- (8) Ganesan, V.; Li, Z.; Wang, X.; Zhang, H. Heterologous Biosynthesis of Natural Product Naringenin by Co-Culture Engineering. *Synth. Syst. Biotechnol.* **2017**, *2* (3), 236–242. https://doi.org/https://doi.org/10.1016/j.synbio.2017.08.003.
- (9) Hwang, E. Il; Kaneko, M.; Ohnishi, Y.; Horinouchi, S. Production of Plant-Specific Flavanones by Escherichia Coli Containing an Artificial Gene Cluster. *Appl. Environ. Microbiol.* **2003**, *69* (5), 2699 LP 2706. https://doi.org/10.1128/AEM.69.5.2699-2706.2003.
- (10) Wu, J.; Yu, O.; Du, G.; Zhou, J. Fine-Tuning of the Fatty Acid Pathway by Synthetic Antisense RNA for Enhanced (2 S)-Naringenin Production from L-Tyrosine in Escherichia Coli. *Appl. Environ. Microbiol.* **2014**, *80* (23), 7283–7292. https://doi.org/10.1128/AEM.02411-14.

- (11) Nicole, C.; Santos, S.; Koffas, M.; Stephanopoulos, G. Optimization of a Heterologous Pathway for the Production of Flavonoids from Glucose. *Metab. Eng.* **2011**, *13* (4), 392–400. https://doi.org/10.1016/j.ymben.2011.02.002.
- (12) Wu, J.; Du, G.; Chen, J.; Zhou, J. Enhancing Flavonoid Production by Systematically Tuning the Central Metabolic Pathways Based on a CRISPR Interference System in Escherichia Coli. *Nat. Publ. Gr.* **2015**, No. February, 1–14. https://doi.org/10.1038/srep13477.
- (13) Jones, J. A.; Vernacchio, V. R.; Sinkoe, A. L.; Collins, S. M.; Ibrahim, M. H. A.; Lachance, D. M.; Hahn, J.; Koffas, M. A. G. Experimental and Computational Optimization of an Escherichia Coli Co-Culture for the Efficient Production of Flavonoids. *Metab. Eng.* **2016**, *35*, 55–63. https://doi.org/https://doi.org/10.1016/j.ymben.2016.01.006.
- (14) Gupta, A.; Reizman, I. M. B.; Reisch, C. R.; Prather, K. L. J. Dynamic Regulation of Metabolic Flux in Engineered Bacteria Using a Pathway-Independent Quorum-Sensing Circuit. *Nat. Biotechnol.* **2017**, *3* (February). https://doi.org/10.1038/nbt.3796.
- (15) Kim, E.-M.; Min Woo, H.; Tian, T.; Yilmaz, S.; Javidpour, P.; Keasling, J. D.; Soon Lee, T. Autonomous Control of Metabolic State by a Quorum Sensing (QS)-Mediated Regulator for Bisabolene Production in Engineered E. Coli. *Metab. Eng.* **2017**, *44* (July), 325–336. https://doi.org/10.1016/j.ymben.2017.11.004.
- (16) Dinh, C. V.; Prather, K. L. J. Development of an Autonomous and Bifunctional Quorum-Sensing Circuit for Metabolic Flux Control in Engineered Escherichia Coli. *Proc. Natl. Acad. Sci.* **2019**, *116* (15), 25562–25568.
- (17) Soma, Y.; Hanai, T. Self-Induced Metabolic State Switching by a Tunable Cell Density Sensor for Microbial Isopropanol Production. *Metab. Eng.* **2015**, *30*, 7–15. https://doi.org/10.1016/j.ymben.2015.04.005.
- (18) You, L.; Cox, R. S.; Weiss, R.; Arnold, F. H. Programmed Population Control by Cell–Cell Communication and Regulated Killing. *Nature* **2004**, *428* (6985), 868–871. https://doi.org/10.1038/nature02491.
- (19) Stephens, K.; Pozo, M.; Tsao, C.-Y.; Hauk, P.; Bentley, W. E. Bacterial Co-Culture with Cell Signaling Translator and Growth Controller Modules for Autonomously Regulated Culture Composition. *Nat. Commun.* **2019**, *10* (1), 4129. https://doi.org/10.1038/s41467-019-12027-6.
- (20) Balagaddé, F. K.; Song, H.; Ozaki, J.; Collins, C. H.; Barnet, M.; Arnold, F. H.; Quake, S. R.; You, L. A Synthetic Escherichia Coli Predator–Prey Ecosystem. *Mol. Syst. Biol.* **2008**, *4* (1), 187. https://doi.org/10.1038/msb.2008.24.
- (21) Gamby, S.; Roy, V.; Guo, M.; Smith, J. A. I.; Wang, J.; Stewart, J. E.; Wang, X.; Bentley, W. E.; Sintim, H. O. Altering the Communication Networks of Multispecies Microbial Systems Using a Diverse Toolbox of AI-2 Analogues. *ACS Chem. Biol.* **2012**, *7* (6), 1023–1030. https://doi.org/10.1021/cb200524y.
- (22) Terrell, J. L.; Wu, H.-C.; Tsao, C.-Y.; Barber, N. B.; Servinsky, M. D.; Payne, G. F.; Bentley, W. E. Nano-Guided Cell Networks as Conveyors of Molecular Communication. *Nat. Commun.* **2015**, *6* (1), 8500. https://doi.org/10.1038/ncomms9500.
- (23) Chen, Y.; Kim, J. K.; Hirning, A. J.; Josić, K.; Bennett, M. R. Emergent Genetic Oscillations in a Synthetic Microbial Consortium. *Science* (80-.). **2015**, 349 (6251), 986 LP 989. https://doi.org/10.1126/science.aaa3794.
- (24) Marchand, N.; Collins, C. H. Synthetic Quorum Sensing and Cell-Cell Communication in

- Gram-Positive Bacillus Megaterium. *ACS Synth. Biol.* **2016**, *5* (7), 597–606. https://doi.org/10.1021/acssynbio.5b00099.
- (25) Kong, W.; Meldgin, D. R.; Collins, J. J.; Lu, T. Designing Microbial Consortia with Defined Social Interactions. *Nat. Chem. Biol.* **2018**, *14* (8), 821–829. https://doi.org/10.1038/s41589-018-0091-7.
- (26) Honjo, H.; Iwasaki, K.; Soma, Y.; Tsuruno, K.; Hamada, H.; Hanai, T. Synthetic Microbial Consortium with Specific Roles Designated by Genetic Circuits for Cooperative Chemical Production. *Metab. Eng.* **2019**, *55*, 268–275. https://doi.org/https://doi.org/10.1016/j.ymben.2019.08.007.
- (27) Brockman, I. M.; Prather, K. L. J. Dynamic Knockdown of E. Coli Central Metabolism for Redirecting Fluxes of Primary Metabolites. *Metab. Eng.* **2015**, *28*, 104–113. https://doi.org/10.1016/j.ymben.2014.12.005.
- (28) Leonard, E.; Lim, K.-H.; Saw, P.-N.; Koffas, M. A. G. Engineering Central Metabolic Pathways for High-Level Flavonoid Production in Escherichia Coli. *Appl. Environ. Microbiol.* **2007**, *73* (12), 3877 LP 3886. https://doi.org/10.1128/AEM.00200-07.
- (29) Leonard, E.; Yan, Y.; Fowler, Z. L.; Li, Z.; Lim, C.-G.; Lim, K.-H.; Koffas, M. A. G. Strain Improvement of Recombinant Escherichia Coli for Efficient Production of Plant Flavonoids. *Mol. Pharm.* **2008**, *5* (2), 257–265. https://doi.org/10.1021/mp7001472.
- (30) Xu, P.; Ranganathan, S.; Fowler, Z. L.; Maranas, C. D.; Koffas, M. A. G. Genome-Scale Metabolic Network Modeling Results in Minimal Interventions That Cooperatively Force Carbon Flux towards Malonyl-CoA. *Metab. Eng.* **2011**, *13* (5), 578–587. https://doi.org/https://doi.org/10.1016/j.ymben.2011.06.008.
- (31) St-Pierre, F.; Cui, L.; Priest, D. G.; Endy, D.; Dodd, I. B.; Shearwin, K. E. One-Step Cloning and Chromosomal Integration of DNA. *ACS Synth. Biol.* **2013**, 537–541.
- (32) Shiue, E. Improvement of D-Glucaric Acid Production in Escherichia Coli, Massachusetts Institute of Technology, 2014.

For Table of Contents Use Only

Development of a quorum-sensing based circuit for control of coculture population composition in a naringenin production system

Christina V. Dinh, Xingyu Chen, Kristala L. J. Prather

